AIAA 81-0603R

# Application of Transonic Codes to Flutter Analysis of Conventional and Supercritical Airfoils

T. Y. Yang*
*Purdue University, W. Lafayette, Ind.*
P. Guruswamy†
*Informatics, Inc., Palo Alto, Calif.*
and
Alfred G. Striz‡
*University of Oklahoma, Norman, Okla.*

**Transonic flutter analyses are performed for two conventional airfoils, NACA 64A006 and NACA 64A010, and three supercritical airfoils, MBB A-3, CAST 7, and the NASA TF-8A wing section at 65.3% semispan. Two degrees of freedom, plunging and pitching about the quarter-chord axis, are considered. The aerodynamic data are obtained by using the two transonic aerodynamics codes LTRAN2 (indicial and time integration methods) and STRANS2/UTRANS2 (harmonic analysis method). The unsteady aerodynamic data are computed within the low reduced frequency range. For all airfoils, the effect of Mach number on flutter speed is studied for several values of four different aeroelastic parameters. For the MBB A-3 supercritical airfoil, the effect of angle of attack on flutter speed is studied. For the cases of a flat plate and a NACA 64A006 airfoil, time response results are obtained by LTRAN2. Applicability and limitations of the two transonic codes are evaluated. Results for the transonic flutter characteristics of these airfoils are discussed and some comparisons are made.**

## Nomenclature

$a_h$ = distance in semichords measured from midchord to elastic axis
$b,c$ = semichord and full-chord lengths, respectively
$C_{lh}$ = lift coefficient due to plunging
$C_{l\alpha}$ = lift coefficient due to pitching
$C_{mh}$ = moment coefficient due to plunging
$C_{m\alpha}$ = moment coefficient due to pitching
$e$ = distance in chords measured from leading edge to center of pressure
$g$ = structural damping coefficient
$h$ = plunging degree of freedom
$I_\alpha$ = polar moment of inertia about elastic axis
$k_b,k_c$ = reduced frequencies defined as $\omega b/U$ and $\omega c/U$, respectively
$m$ = mass of the airfoil per unit span
$r_\alpha$ = radius of gyration about elastic axis = $(I_\alpha/mb^2)^{1/2}$
$S$ = airfoil static moment about elastic axis
$U$ = freestream velocity
$x_p$ = distance in semichords measured from midchord to pitching axis
$x_\alpha$ = distance in semichords measured from elastic axis to mass center = $S/mb$
$\alpha$ = pitching degree of freedom
$\mu$ = airfoil-air mass density ratio = $m/\pi\rho b^2$
$\rho$ = freestream air density
$\omega$ = flutter frequency
$\omega_h$ = uncoupled plunging frequency
$\omega_\alpha$ = uncoupled pitching frequency
$\omega_r$ = reference frequency set equal to unity

Presented as Paper 81-0603 at the AIAA Dynamics Specialist Conference, Atlanta, Ga., April 9-10, 1981; submitted April 24, 1981; revision received July 21, 1981. 

*Professor and Head, School of Aeronautics and Astronautics. Associate Fellow AIAA.
†Research Scientist. Member AIAA.
‡Assistant Professor, School of Aerospace, Mechanical, and Nuclear Engineering. Formerly Research Assistant, Purdue University. Member AIAA.

## Introduction

In recent years, there has been extensive progress in transonic unsteady computational aerodynamics. A review of the state-of-the-art of the numerical methods was given by Ballhaus and Bridgeman.[1] Based on the developments in computational aerodynamics, aeroelastic applications have been performed and were reviewed by Ashley.[2] In the present study, the applications of transonic codes to flutter analyses of conventional and supercritical airfoils are discussed as a summary of three years of research sponsored by the Air Force Office of Scientific Research.

To date, a number of efficient transonic computer codes are available to solve the two-dimensional, inviscid, small-disturbance, unsteady aerodynamic equations by the finite difference method.

Traci, Albano, and Farr[3] developed the codes STRANS2 and UTRANS2 to solve the transonic steady and unsteady equations by the relaxation method. The unsteady equation is time-linearized by treating the unsteady solution as a small linear harmonic perturbation about a nonlinear steady-state solution.

Ballhaus and Goorjian[4] used a time integration method to solve the unsteady transonic equation. They developed the code LTRAN2 to time-accurately solve the low-frequency transonic equations. This code accounts for shock movement during the unsteady computations. The code also includes an indicial method. Recently, several modifications have been incorporated into LTRAN2. Houwink and van der Vooren[5] modified LTRAN2 by adding high-frequency terms to the boundary conditions and pressure computations. Recently, Rizzetta and Yoshihara[6] developed an unsteady transonic code, ExTRAN2, which does not have any low-frequency assumptions. High-frequency terms are retained in the potential equations, the boundary conditions, and the pressure computations. Viscous effects are incorporated in the program by using a viscous ramp method.

Goorjian[7] did a preliminary study to remove the small-disturbance and low-frequency restrictions by considering the full potential equations. Williams[8] discussed a procedure of linearizing unsteady transonic flows which contain shocks. He

considered the equations governing the unsteady field, allowing for induced oscillations of any embedded shocks.

In addition to these finite difference methods, several other methods such as the finite element method and the Kernel function method have been applied to solve the unsteady transonic equations. A brief survey of such efforts is given in Ref. 9.

There have also been attempts to solve the three-dimensional, inviscid, small-disturbance transonic equations. Traci, Albano, and Farr[3] developed the codes TDSTRN and TDUTRN utilizing the relaxation method. Recently, Borland, Rizzetta, and Yoshihara[10] presented a transonic code, LTRAN3, which solves the three-dimensional, low-frequency, unsteady transonic equation by time integration method.

Parallel to these theoretical attempts, several experimental studies have been conducted in the area of transonic aerodynamics. In Ref. 11, steady-state wind-tunnel results are presented for several supercritical airfoils. Tijdeman[12] undertook steady and unsteady wind-tunnel experiments on a NACA 64A006 airfoil. Davis and Malcolm[13] studied the aerodynamic characteristics of an oscillating NACA 64A010 airfoil in the wind tunnel at transonic Mach numbers. Davis and Malcolm[14] also obtained experimental unsteady aerodynamic results for the NACA 64A010 conventional airfoil and the NLR 7301 supercritical airfoil.

Based on the theoretical and experimental developments in unsteady transonic aerodynamics, aeroelastic applications have been investigated. In Ref. 3, Traci, Albano, and Farr reported a flutter analysis of the NACA 64A006 and NACA 64A410 airfoils based on aerodynamic coefficients computed by the relaxation programs STRANS2 and UTRANS2. Preliminary results obtained for the NACA 64A006 airfoil demonstrated the importance of the transonic range by the drop in flutter speed at $M=0.85$. The restricted Mach number range of the aerodynamic data did not permit an in-depth examination of the NACA 64A410 airfoil. Rizzetta[15] performed flutter analysis of a NACA 64A010 airfoil by using the same two programs, STRANS2 and UTRANS2. He also reported an aeroelastic time response analysis for this airfoil.[16] Two cases, single (pitch) and three (pitch, plunge, and aileron pitch) degrees of freedom, were considered.

Ballhaus and Goorjian[17] used the time integration and indicial approaches to conduct aeroelastic response analyses. They presented a time response procedure to determine the flutter speed of a single-pitching-degree-of-freedom NACA 64A006 airfoil at $M=0.88$. The response histories were computed by using LTRAN2 coupled with a simple ordinary differential equation integration procedure such that the aerodynamic equation and the equation of motion of the airfoil were integrated simultaneously.

In Ref. 2, Ashley studied flutter characteristics of the TF-8A wing section at the 65.3% semispan station by using experimental wind-tunnel data. McGrew et al.[18] carried out transonic flutter analysis of supercritical wings, studying a TF-8A flutter model and the YC-15II prototype aircraft.

Mykytow[19] pointed out the detrimental effect of mass ratio on the flutter boundary in the transonic region: the greater the mass ratio, the deeper the dip. From the study of a binary system of the streamwise section of a sweptback wing, Isogai[20] concluded that the mechanism of the single-degree-of-freedom flutter dominates the flutter of the system studied at the bottom of the transonic dip. He also remarked that the large time lag between the aerodynamic pressures and the airfoil motion in the transonic region, caused by the compressibility effect, is the main cause of the transonic dip phenomenon. Recently, Isogai[21] conducted an extensive transonic flutter analysis of a NACA 64A010 airfoil. Flutter calculations were performed for two typical binary systems, one simulating the vibrational characteristics of a typical streamwise section of a sweptback wing, and the other those of an unswept wing. A sharp transonic dip of the flutter boundary is shown for the former case, while the dip for the latter is relatively mild. Once again, he concluded that the mechanism of the single-degree-of-freedom flutter, which is caused by the large negative damping produced by the phase lag of the shock wave motion, dominates the flutter at the bottom of the transonic dip when the mass ratio is relatively large.

In a Comment by Hitch and the Reply by Yang et al.,[22] it was explained that transonic flutter speed is affected by the magnitude of lift coefficient $C_{l\alpha}$ and the aft-movement of the center of pressure. The former decreases the flutter speed, whereas the latter increases the flutter speed.

Farmer and Hanson[23] performed a wind-tunnel study to investigate the flutter behavior of two dynamically similar wings, one with supercritical wing sections and the other with conventional ones. It was found that the supercritical wing experienced a much more pronounced transonic dip than the conventional wing.

Eastep and Olsen[24] reported the flutter analysis of a rectangular wing by using the three-dimensional unsteady transonic codes TDSTRN and TDUTRN.[3] With increase in Mach number, both flutter speed and frequency decreased in the transonic regime. The decrease in flutter speed was greater when transonic aerodynamics were used as compared to linear aerodynamics.

In this study, flutter analyses were performed for five airfoils, oscillating in plunge and pitch about the quarter-chord axis. For the two conventional airfoils NACA 64A006 and NACA 64A010 and the supercritical airfoil MBB A-3, both LTRAN2 and STRANS2/UTRANS2 were simultaneously employed to obtain the aerodynamic data. For the other two supercritical airfoils, CAST 7 and the NASA TF-8A wing section at the 65.3% semispan station, the aerodynamic data were obtained by LTRAN2 and STRANS2/UTRANS2, respectively. Four aeroelastic parameters were considered as variables in the analyses: the airfoil-air mass density ratio, the position of the mass center, the plunge-to-pitch frequency ratio, and the position of the elastic axis.

The effect of Mach number on flutter speed was studied for various values of these parameters. The transonic dip phenomenon was illustrated and explained. For the MBB A-3 supercritical airfoil, the effects of angle of attack, camber, and supercritical thickness distribution on flutter speed were also examined.

Time response results were obtained for a flat plate and a NACA 64A006 airfoil by simultaneously integrating the LTRAN2 aerodynamic equations and the structural equations. Both a single- and a two-degree-of-freedom case were considered. Neutrally stable response was found when checking a lowest point on the transonic flutter speed curve.

Applicability and limitations of the two transonic codes are evaluated. Results obtained for the transonic flutter

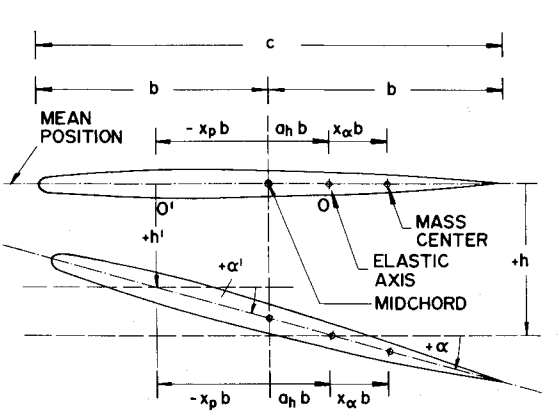


**Fig. 1 Definition of parameters for a 2-degree-of-freedom aeroelastic system.**

characteristics of these airfoils are discussed and some comparisons are made.

## Aeroelastic Equations of Motion

Figure 1 defines the sign conventions and the parameters for a typical airfoil oscillating in pitch and plunge. The system is similar to that shown in Sec. 9-2 of Ref. 25.

In deriving the equations, the assumptions were 1) displacement $h$ and rotation $\alpha$ are measured from the mean position given by the steady-state condition; 2) the airfoil is rigid; 3) the amplitudes of oscillation are assumed to be small; and 4) the principle of superposition of airloads holds even when there are shocks present. Discussion and justification of the last assumption were given in Ref. 13.

Considering equilibrium of the aeroelastic system as shown in Fig. 1, the final eigenvalue equations for flutter analysis are[9]

$$(\mu k_b^2[M]-[A])\begin{Bmatrix}\xi_0\\ \alpha_0\end{Bmatrix}=\lambda[K]\begin{Bmatrix}\xi_0\\ \alpha_0\end{Bmatrix} \tag{1}$$

where $\xi_0$ and $\alpha_0$ are the nondimensional amplitudes in plunge and pitch oscillations, respectively; $\mu$ and $k_b$ are defined in the Nomenclature.

The matrices $[M]$, $[A]$, and $[K]$ are as follows:

$$[M]=\left[\begin{array}{c|c} 1 & x_\alpha \\ \hline x_\alpha & r_\alpha^2 \end{array}\right] \tag{2a}$$

$$[A]=\frac{1}{\pi}\left[\begin{array}{c|c} C_{lh}/2 & C_{l\alpha} \\ \hline -C_{mh} & -2C_{m\alpha} \end{array}\right] \tag{2b}$$

$$[K]=\left[\begin{array}{c|c} (\omega_h/\omega_r)^2 & 0 \\ \hline 0 & r_\alpha^2(\omega_\alpha/\omega_r)^2 \end{array}\right] \tag{2c}$$

The eigenvalue $\lambda$ is complex and defined as

$$\lambda=\mu(1+ig)\omega_r^2b^2/U^2 \tag{3}$$

where $g$ represents the structural damping coefficient, which is assumed to be small and of the same order for both plunging and pitching modes. A flutter solution is obtained when $g$ is found to be zero. In the transonic flutter analysis, the essential task is the computation of the aerodynamic coefficients for Eq. (2b).

## Results and Discussions

The equations for the configurations of the five airfoils studied were supplied by Olsen.[26] The airfoil data are presented in Ref. 27, except for the TF-8A wing section, for which the data are given in Ref. 28. Figure 2 shows the configurations of all the airfoils considered.

### Flutter Analysis of a NACA 64A006 Airfoil

Detailed flutter analyses were first performed for the conventional NACA 64A006 airfoil (6% thickness-to-chord ratio) and are given in Refs. 9, 22, and 29. The airfoil was assumed to plunge and pitch about the quarter-chord axis. The aerodynamic coefficients were obtained for $M=0.7$, 0.8, 0.85, 0.8625, and 0.87, in the low reduced frequency range. Both computer codes STRANS2/UTRANS2 and LTRAN2 were employed. Flutter results were presented as plots of flutter speed and the corresponding reduced frequency vs airfoil-air mass density ratio, position of mass center, position of elastic axis, or freestream Mach number. In each figure, several sets of curves for different values of plunge-to-pitch frequency ratio were shown. The effects of these parameters on the flutter characteristics of this airfoil were discussed.

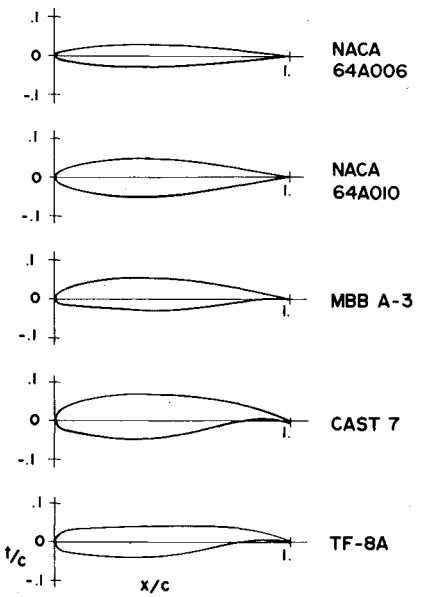


Fig. 2 Airfoil configurations.

The two sets of results based on the two separate computer codes were, in general, in good agreement. Flutter results of the transonic codes compared well with those obtained by linear flate plate theory in the subsonic regime. However, only the transonic codes presented the transonic dip near $M=0.85$.

### Flutter Analysis of a NACA 64A010 Airfoil

Flutter analyses were performed for the NACA 64A010 conventional airfoil (10% thickness-to-chord ratio) and are given in Ref. 9. The aerodynamic coefficients were obtained for plunge and pitch about the quarter-chord axis at $M=0.72$, 0.76, and 0.80, and at various values of low reduced frequency. Both computer programs, LTRAN2 in the indicial mode and STRANS2/UTRANS2, were used. Flutter results were presented as plots of flutter speed and the corresponding reduced frequency vs each of the three aeroelastic parameters ($\mu$, $x_\alpha$, $a_h$) or freestream Mach number. In each figure, several sets of curves for different values of plunge-to-pitch frequency ratio were shown.

The effects of the aeroelastic parameters on the flutter characteristics of this airfoil were discussed. The two sets of results obtained in Ref. 9 based on the two computer codes were, in general, in good agreement.

Additional results which were not given in Ref. 9 are obtained here for $M=0.82$ by LTRAN2 and STRANS2/UTRANS2. Results for flutter speed and reduced frequency vs Mach number are given in Fig. 3 for three $\mu$-values. All the curves show a transonic dip. The minimum for the two curves by the indicial method for $\mu=200$ and 300 appears to be at $M>0.82$. The detrimental effect of the mass ratio is seen: the higher the $\mu$, the deeper the dip.

### Flutter Analysis of a MBB A-3 Supercritical Airfoil

Detailed analyses of a MBB A-3 supercritical airfoil were conducted to study 1) the flutter characteristics of the airfoil at 0-deg angle of attack and design Mach number 0.765; 2) the flutter characteristics of the airfoil at design Mach number and design $C_l=0.58$; 3) the effect of camber on its flutter characteristics; 4) the comparison with flutter characteristics of a conventional symmetric airfoil of the same thickness-to-chord ratio; 5) the effect of Mach number on its flutter speed; and 6) the effect of angle of attack on flutter speed. Studies 1-5 were reported in Refs. 30 and 31.

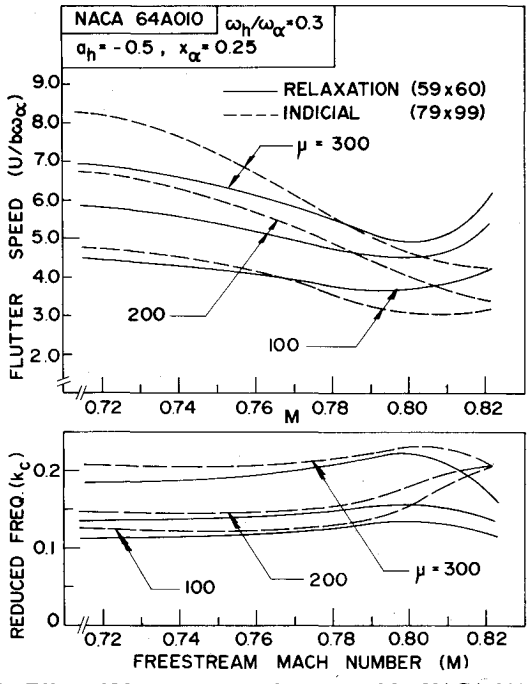


Fig. 3 Effect of Mach number on flutter speed for NACA 64A010.

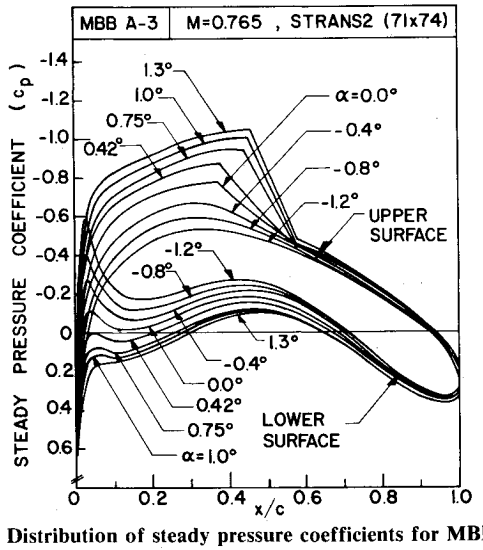


Fig. 4 Distribution of steady pressure coefficients for MBB A-3 by STRANS2.

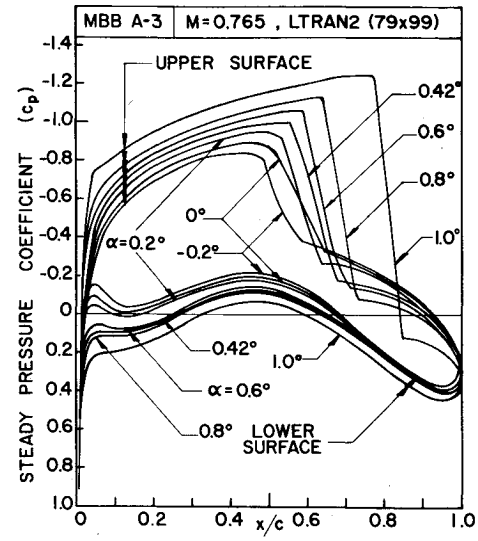


Fig. 5 Distribution of steady pressure coefficients for MBB A-3 by LTRAN2.

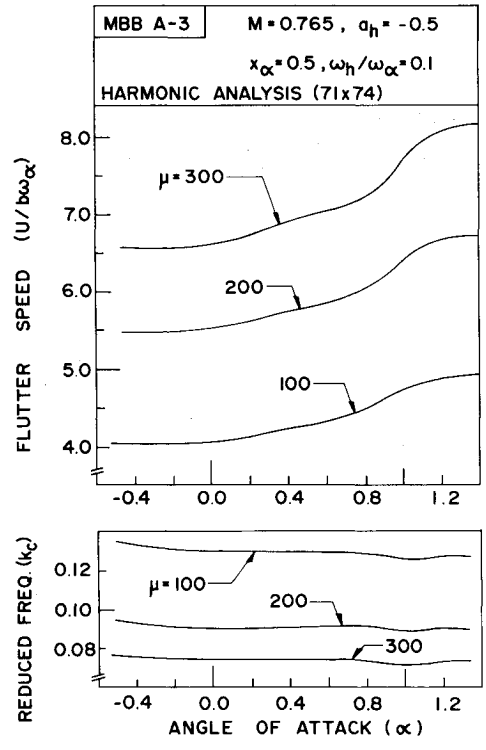


Fig. 6 Effect of angle of attack on flutter speed for MBB A-3 by STRANS2/UTRANS2.

The aerodynamic coefficients were obtained by using both codes STRANS2/UTRANS2 and LTRAN2 for these six studies. Flutter results were presented as plots of flutter speed vs different aeroelastic parameters, Mach number, or angle of attack.

In study 1, the aerodynamic and flutter results obtained by the two codes at $M=0.765$ and $\alpha=0.0$ deg compared well. They also provided a basis for comparison with later results.

In study 2, flutter analysis was conducted at design Mach number 0.765 and the equivalent design angle of attack that yields a design lift coefficient of $C_l=0.58$. These angles were 0.75 and 0.42 deg for STRANS2 and LTRAN2, respectively. In general, the airfoil was more stable at the equivalent design angle of attack than at 0-deg angle of attack.

In study 3, flutter analysis was carried out for a MBB A-3 supercritical airfoil without camber at design Mach number and the equivalent design angles of attack. Within the range of values selected for all parameters, removal of the camber from the airfoil decreased the flutter speed; i.e., the camber had a stabilizing effect on the airfoil.

In study 4, a conventional airfoil, NACA 64A010, was scaled down to the same maximum thickness-to-chord ratio as the MBB A-3 airfoil (8.9%). The flutter characteristics of this equivalent conventional airfoil were almost the same as those of the MBB A-3 airfoil without camber.

In study 5, the effect of Mach number on flutter characteristics of the MBB A-3 airfoil at 0-deg angle of attack was investigated. The Mach numbers considered were 0.70, 0.72, 0.74, 0.765, and 0.78, respectively. All the curves for flutter speed showed a dip in the neighborhood of the transonic design Mach number $M=0.765$. The effects of $x_\alpha$, $\mu$, $\omega_h/\omega_\alpha$, and $a_h$ on the various characteristics of the dip phenomenon were demonstrated.

In study 6, steady and unsteady aerodynamic results were computed for the MBB A-3 supercritical airfoil for various angles of attack at the design Mach number. Because of

**Table 1 Aerodynamic coefficients for MBB A-3 for various angles of attack at $M = 0.765$ by UTRANS2**

| | | Reduced frequency, $k_c$ | | | | | | | | | |
|---|---|---|---|---|---|---|---|---|---|---|---|
| | Angle of attack, deg | 0.0 | | 0.05 | | 0.10 | | 0.15 | | 0.20 | |
| | | Re | Im | Re | Im | Re | Im | Re | Im | Re | Im |
| $C_{l\delta}$ | 1.3 | ... | ... | 0.104 | 0.492 | 0.278 | 0.835 | 0.492 | 1.074 | 0.677 | 1.184 |
| | 1.2 | ... | ... | 0.106 | 0.499 | 0.281 | 0.844 | 0.501 | 1.087 | 0.695 | 1.197 |
| | 1.0 | ... | ... | 0.111 | 0.508 | 0.285 | 0.854 | 0.508 | 1.100 | 0.710 | 1.209 |
| | 0.75 | ... | ... | 0.119 | 0.557 | 0.279 | 0.906 | 0.539 | 1.172 | 0.772 | 1.277 |
| | 0.42 | ... | ... | 0.094 | 0.513 | 0.286 | 0.881 | 0.536 | 1.138 | 0.745 | 1.262 |
| | 0 | ... | ... | 0.089 | 0.521 | 0.260 | 0.900 | 0.523 | 1.185 | 0.772 | 1.288 |
| | −0.4 | ... | ... | 0.091 | 0.512 | 0.281 | 0.881 | 0.521 | 1.150 | 0.736 | 1.275 |
| $C_{l\alpha}$ | 1.3 | 10.376 | 0 | 9.345 | −1.724 | 8.254 | −2.451 | 7.260 | −2.718 | 6.362 | −2.747 |
| | 1.2 | 10.590 | 0 | 9.514 | −1.768 | 8.389 | −2.521 | 7.360 | −2.808 | 6.435 | −2.839 |
| | 1.0 | 10.709 | 0 | 9.610 | −1.803 | 8.463 | −2.567 | 7.419 | −2.853 | 6.483 | −2.884 |
| | 0.75 | 11.388 | 0 | 10.171 | −1.941 | 8.932 | −2.818 | 7.757 | −3.144 | 6.702 | −3.180 |
| | 0.42 | 11.168 | 0 | 9.992 | −1.915 | 8.757 | −2.687 | 7.677 | −2.948 | 6.744 | −2.966 |
| | 0 | 11.221 | 0 | 10.141 | −1.949 | 8.843 | −2.801 | 7.667 | −3.060 | 6.710 | −2.970 |
| | −0.4 | 11.129 | 0 | 9.979 | −1.878 | 8.780 | −2.605 | 7.745 | −2.857 | 6.845 | −2.881 |
| $C_{m\delta}$ | 1.3 | ... | ... | −0.007 | −0.044 | −0.016 | −0.077 | −0.031 | −0.106 | −0.051 | −0.125 |
| | 1.2 | ... | ... | −0.006 | −0.043 | −0.016 | −0.076 | −0.029 | −0.106 | −0.050 | −0.126 |
| | 1.0 | ... | ... | −0.005 | −0.040 | −0.012 | −0.071 | −0.023 | −0.100 | −0.040 | −0.121 |
| | 0.75 | ... | ... | −0.003 | −0.035 | −0.003 | −0.060 | −0.009 | −0.090 | −0.020 | −0.113 |
| | 0.42 | ... | ... | 0.0 | −0.024 | 0.002 | −0.047 | 0.002 | −0.072 | 0.0 | −0.096 |
| | 0 | ... | ... | 0.003 | −0.015 | 0.010 | −0.031 | 0.017 | −0.053 | 0.020 | −0.076 |
| | −0.4 | ... | ... | 0.003 | −0.012 | 0.010 | −0.026 | 0.018 | −0.044 | 0.025 | −0.065 |
| $C_{m\alpha}$ | 1.3 | −0.901 | 0 | −0.829 | 0.073 | −0.766 | 0.079 | −0.715 | 0.066 | −0.671 | 0.061 |
| | 1.2 | −0.899 | 0 | −0.826 | 0.069 | −0.764 | 0.073 | −0.715 | 0.059 | −0.673 | 0.052 |
| | 1.0 | −0.824 | 0 | −0.759 | 0.048 | −0.709 | 0.040 | −0.672 | 0.019 | −0.643 | 0.007 |
| | 0.75 | −0.691 | 0 | −0.640 | 0.006 | −0.614 | −0.023 | −0.597 | −0.056 | −0.589 | −0.073 |
| | 0.42 | −0.510 | 0 | −0.482 | −0.032 | −0.472 | −0.087 | −0.476 | −0.140 | −0.489 | −0.180 |
| | 0 | −0.311 | 0 | −0.307 | −0.074 | −0.319 | −0.148 | −0.340 | −0.212 | −0.365 | −0.265 |
| | −0.4 | −0.248 | 0 | −0.246 | −0.082 | −0.262 | −0.162 | −0.285 | −0.231 | −0.314 | −0.286 |

**Table 2 Aerodynamic coefficients for MBB A-3 for various angles of attack at $M = 0.765$ by LTRAN2**

| | | Reduced frequency, $k_c$ | | | | | | | |
|---|---|---|---|---|---|---|---|---|---|
| | Angle of attack, deg | 0.05 | | 0.10 | | 0.15 | | 0.20 | |
| | | Re | Im | Re | Im | Re | Im | Re | Im |
| $C_{l\delta}$ | −0.2 | 0.160 | 0.598 | 0.429 | 1.036 | 0.694 | 1.362 | 0.977 | 1.595 |
| | 0.0 | 0.171 | 0.636 | 0.422 | 1.100 | 0.724 | 1.420 | 0.881 | 1.728 |
| | 0.2 | 0.238 | 0.671 | 0.595 | 1.095 | 0.900 | 1.386 | 1.199 | 1.563 |
| | 0.42 | 0.324 | 0.728 | 0.734 | 1.130 | 1.058 | 1.379 | 1.355 | 1.505 |
| | 0.6 | 0.452 | 0.783 | 0.917 | 1.133 | 1.247 | 1.314 | 1.493 | 1.417 |
| | 0.8 | 0.709 | 0.830 | 1.165 | 1.105 | 1.441 | 1.231 | 1.619 | 1.311 |
| $C_{l\alpha}$ | −0.2 | 11.965 | −3.206 | 10.356 | −4.290 | 9.078 | −4.625 | 7.974 | −4.886 |
| | 0.0 | 12.724 | −3.409 | 11.001 | −4.223 | 9.469 | −4.825 | 8.642 | −4.403 |
| | 0.2 | 13.419 | −4.752 | 10.952 | −5.946 | 9.237 | −5.999 | 7.815 | −5.997 |
| | 0.42 | 14.555 | −6.480 | 11.303 | −7.340 | 9.195 | −7.055 | 7.524 | −6.775 |
| | 0.6 | 15.662 | −9.043 | 11.329 | −9.174 | 8.763 | −8.316 | 7.086 | −7.467 |
| | 0.8 | 16.604 | −14.18 | 11.053 | −11.65 | 8.205 | −9.607 | 6.554 | −8.093 |
| $C_{m\delta}$ | −0.2 | −0.005 | −0.026 | −0.031 | −0.049 | −0.022 | −0.073 | −0.030 | −0.100 |
| | 0.0 | −0.008 | −0.038 | −0.015 | −0.071 | −0.022 | −0.103 | −0.029 | −0.136 |
| | 0.2 | −0.021 | −0.054 | −0.052 | −0.089 | −0.077 | −0.118 | −0.107 | −0.140 |
| | 0.42 | −0.043 | −0.085 | −0.092 | −0.127 | −0.137 | −0.152 | −0.180 | −0.162 |
| | 0.6 | −0.078 | −0.120 | −0.158 | −0.158 | −0.215 | −0.174 | −0.268 | −0.164 |
| | 0.8 | −0.171 | −0.171 | −0.280 | −0.182 | −0.346 | −0.176 | −0.385 | −0.171 |
| $C_{m\alpha}$ | −0.2 | −0.511 | 0.109 | −0.489 | 0.131 | −0.489 | 0.145 | −0.502 | 0.149 |
| | 0.0 | −0.763 | 0.162 | −0.706 | 0.150 | −0.686 | 0.146 | −0.680 | 0.145 |
| | 0.2 | −1.084 | 0.416 | −0.892 | 0.515 | −0.790 | 0.513 | −0.699 | 0.537 |
| | 0.42 | −1.704 | 0.868 | −1.272 | 0.924 | −1.014 | 0.913 | −0.811 | 0.901 |
| | 0.6 | −2.391 | 1.553 | −1.579 | 1.579 | −1.158 | 1.430 | −0.820 | 1.338 |
| | 0.8 | −3.409 | 3.409 | −1.820 | 2.803 | −1.175 | 2.306 | −0.857 | 1.924 |

**Table 3 Aerodynamic coefficients for CAST 7 for various Mach numbers by LTRAN2**

| | Mach No. | Reduced frequency, $k_c$ 0.05 Re | 0.05 Im | 0.10 Re | 0.10 Im | 0.15 Re | 0.15 Im | 0.20 Re | 0.20 Im |
|---|---|---|---|---|---|---|---|---|---|
| | 0.600 | 0.033 | 0.413 | 0.116 | 0.798 | 0.229 | 1.153 | 0.355 | 1.480 |
| | 0.625 | 0.045 | 0.428 | 0.131 | 0.824 | 0.267 | 1.180 | 0.384 | 1.514 |
| | 0.650 | 0.047 | 0.449 | 0.159 | 0.855 | 0.293 | 1.221 | 0.458 | 1.544 |
| $C_{l\delta}$ | 0.675 | 0.063 | 0.480 | 0.192 | 0.904 | 0.359 | 1.272 | 0.542 | 1.597 |
| | 0.700 | 0.088 | 0.553 | 0.285 | 1.051 | 0.532 | 1.387 | 0.759 | 1.705 |
| | 0.710 | 0.132 | 0.620 | 0.391 | 1.103 | 0.698 | 1.463 | 0.999 | 1.730 |
| | 0.720 | 0.258 | 0.759 | 0.653 | 1.241 | 1.047 | 1.523 | 1.372 | 1.695 |
| | 0.600 | 8.263 | −0.650 | 7.976 | −1.156 | 7.685 | −1.529 | 7.402 | −1.777 |
| | 0.625 | 8.566 | −0.900 | 8.237 | −1.305 | 7.864 | −1.780 | 7.568 | −1.922 |
| | 0.650 | 8.987 | −0.945 | 8.549 | −1.585 | 8.139 | −1.954 | 7.722 | −2.288 |
| $C_{l\alpha}$ | 0.675 | 9.593 | −1.263 | 9.037 | −1.921 | 8.483 | −2.392 | 7.986 | −2.711 |
| | 0.700 | 11.047 | −1.750 | 10.513 | −2.854 | 9.245 | −3.549 | 8.527 | −3.797 |
| | 0.710 | 12.400 | −2.636 | 11.030 | −3.906 | 9.753 | −4.652 | 8.652 | −4.995 |
| | 0.720 | 15.176 | −5.152 | 12.407 | −6.528 | 10.150 | −6.977 | 8.473 | −6.862 |
| | 0.600 | 0.001 | −0.001 | 0.003 | −0.003 | 0.007 | −0.005 | 0.011 | −0.008 |
| | 0.625 | 0.001 | −0.001 | 0.004 | −0.003 | 0.008 | −0.005 | 0.014 | −0.009 |
| | 0.650 | 0.002 | −0.001 | 0.006 | −0.003 | 0.012 | −0.005 | 0.018 | −0.009 |
| $C_{m\delta}$ | 0.675 | 0.004 | 0.004 | 0.009 | 0.002 | 0.018 | −0.001 | 0.028 | −0.007 |
| | 0.700 | 0.005 | −0.001 | 0.016 | −0.003 | 0.031 | −0.013 | 0.047 | −0.027 |
| | 0.710 | 0.006 | −0.021 | 0.015 | −0.040 | 0.026 | −0.063 | 0.025 | −0.091 |
| | 0.720 | −0.011 | −0.085 | −0.040 | −0.147 | −0.078 | −0.189 | −0.119 | −0.218 |
| | 0.600 | −0.021 | −0.020 | −0.026 | −0.034 | −0.030 | −0.046 | −0.039 | −0.057 |
| | 0.625 | −0.023 | −0.024 | −0.027 | −0.040 | −0.036 | −0.056 | −0.047 | −0.068 |
| | 0.650 | −0.015 | −0.032 | −0.025 | −0.059 | −0.032 | −0.077 | −0.046 | −0.091 |
| $C_{m\alpha}$ | 0.675 | 0.070 | −0.074 | 0.022 | −0.093 | −0.003 | −0.117 | −0.034 | −0.140 |
| | 0.700 | −0.009 | −0.089 | −0.030 | −0.162 | −0.085 | −0.205 | −0.137 | −0.237 |
| | 0.710 | −0.414 | −0.111 | −0.399 | −0.153 | −0.417 | −0.173 | −0.457 | −0.123 |
| | 0.720 | −1.705 | 0.225 | −1.472 | 0.395 | −1.261 | 0.522 | −1.092 | 0.593 |

**Table 4 Aerodynamic coefficients for TF-8A at $\alpha = -3.0$ deg for various Mach numbers by UTRANS2**

| | Mach No. | Reduced frequency, $k_c$ 0.0 Re | 0.0 Im | 0.05 Re | 0.05 Im | 0.10 Re | 0.10 Im | 0.15 Re | 0.15 Im | 0.20 Re | 0.20 Im |
|---|---|---|---|---|---|---|---|---|---|---|---|
| | 0.70 | 0.0 | 0 | 0.057 | 0.471 | 0.218 | 0.828 | 0.395 | 1.094 | 0.549 | 1.312 |
| | 0.74 | 0.0 | 0 | 0.081 | 0.485 | 0.251 | 0.844 | 0.453 | 1.104 | 0.619 | 1.290 |
| | 0.76 | 0.0 | 0 | 0.088 | 0.496 | 0.279 | 0.864 | 0.494 | 1.113 | 0.668 | 1.268 |
| $C_{l\delta}$ | 0.77 | 0.0 | 0 | 0.095 | 0.513 | 0.299 | 0.889 | 0.531 | 1.138 | 0.722 | 1.276 |
| | 0.78 | 0.0 | 0 | 0.108 | 0.535 | 0.335 | 0.909 | 0.574 | 1.132 | 0.752 | 1.283 |
| | 0.79 | 0.0 | 0 | 0.105 | 0.510 | 0.323 | 0.858 | 0.543 | 1.067 | 0.697 | 1.201 |
| | 0.80 | 0.0 | 0 | 0.113 | 0.516 | 0.340 | 0.854 | 0.555 | 1.057 | 0.706 | 1.186 |
| | 0.70 | 9.444 | 0 | 9.430 | −0.634 | 8.219 | −1.674 | 7.568 | −1.941 | 6.971 | −2.043 |
| | 0.74 | 10.174 | 0 | 9.358 | −1.462 | 8.455 | −2.095 | 7.629 | −2.368 | 6.886 | −2.438 |
| | 0.76 | 10.631 | 0 | 9.649 | −1.689 | 8.581 | −2.376 | 7.634 | −2.631 | 6.796 | −2.661 |
| $C_{l\alpha}$ | 0.77 | 11.161 | 0 | 10.034 | −1.876 | 8.840 | −2.640 | 7.776 | −2.893 | 6.851 | −2.891 |
| | 0.78 | 11.768 | 0 | 10.440 | −2.141 | 9.068 | −2.917 | 7.904 | −3.156 | 6.889 | −3.130 |
| | 0.79 | 11.236 | 0 | 9.904 | −2.056 | 8.560 | −2.761 | 7.436 | −2.934 | 6.486 | −2.861 |
| | 0.80 | 11.366 | 0 | 9.939 | −2.124 | 8.552 | −2.843 | 7.394 | −3.013 | 6.424 | −2.932 |
| | 0.70 | 0.0 | 0 | 0.004 | −0.001 | 0.011 | −0.004 | 0.022 | −0.012 | 0.035 | −0.021 |
| | 0.74 | 0.0 | 0 | 0.003 | −0.007 | 0.010 | −0.015 | 0.019 | −0.026 | 0.029 | −0.039 |
| | 0.76 | 0.0 | 0 | 0.002 | −0.012 | 0.007 | −0.026 | 0.014 | −0.040 | 0.021 | −0.056 |
| $C_{m\delta}$ | 0.77 | 0.0 | 0 | 0.002 | −0.015 | 0.006 | −0.029 | 0.012 | −0.046 | 0.018 | −0.063 |
| | 0.78 | 0.0 | 0 | 0.001 | −0.016 | 0.006 | −0.032 | 0.011 | −0.049 | 0.018 | −0.066 |
| | 0.79 | 0.0 | 0 | −0.002 | −0.030 | −0.005 | −0.054 | −0.008 | −0.075 | −0.007 | −0.094 |
| | 0.80 | 0.0 | 0 | −0.006 | −0.042 | −0.018 | −0.073 | −0.028 | −0.096 | −0.033 | −0.116 |
| | 0.70 | −0.013 | 0 | −0.019 | −0.096 | −0.042 | −0.170 | −0.066 | −0.240 | −0.090 | −0.301 |
| | 0.74 | −0.115 | 0 | −0.122 | −0.086 | −0.139 | −0.165 | −0.161 | −0.234 | −0.184 | −0.293 |
| | 0.76 | −0.238 | 0 | −0.235 | −0.070 | −0.243 | −0.143 | −0.256 | −0.209 | −0.273 | −0.266 |
| $C_{m\alpha}$ | 0.77 | −0.285 | 0 | −0.277 | −0.065 | −0.283 | −0.136 | −0.293 | −0.203 | −0.307 | −0.262 |
| | 0.78 | −0.311 | 0 | −0.301 | −0.066 | −0.305 | −0.141 | −0.316 | −0.209 | −0.331 | −0.270 |
| | 0.79 | −0.611 | 0 | −0.560 | −0.003 | −0.522 | −0.042 | −0.499 | −0.099 | −0.484 | −0.163 |
| | 0.80 | −0.890 | 0 | −0.797 | 0.073 | −0.718 | 0.057 | −0.658 | 0.011 | −0.615 | −0.059 |

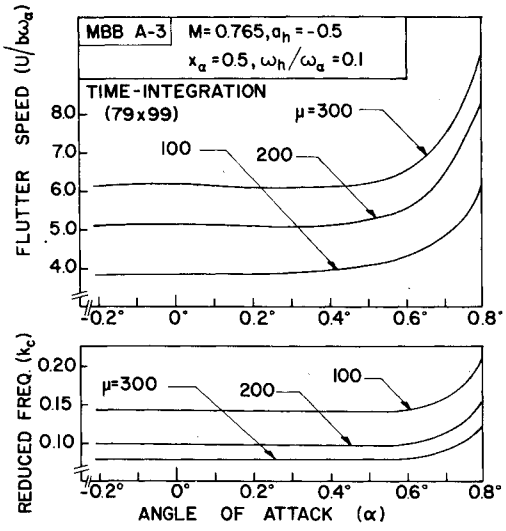


Fig. 7 Effect of angle of attack on flutter speed for MBB A-3 by LTRAN2.

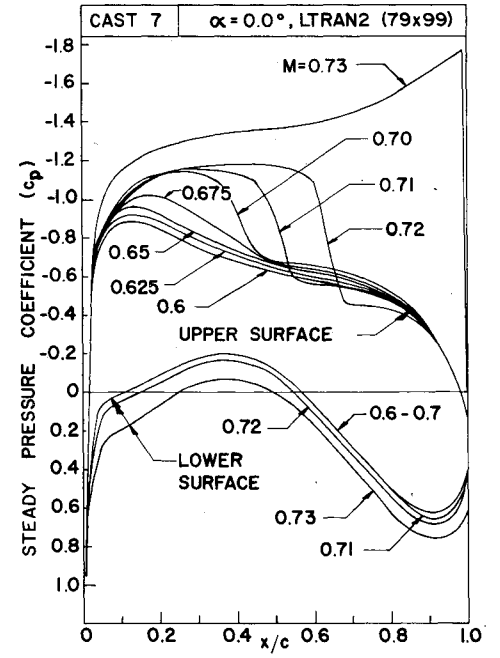


Fig. 8 Distribution of steady pressure coefficients for CAST 7 by LTRAN2.

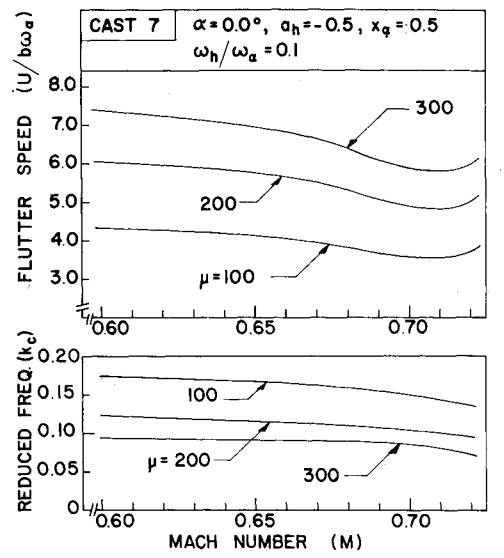


Fig. 9 Effect of Mach number on flutter speed for CAST 7 by LTRAN2.

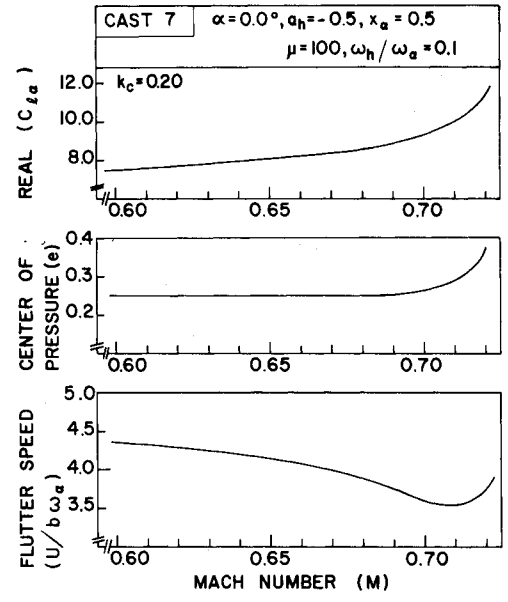


Fig. 10 Compensating effects of Re ($C_{l\alpha}$) and $e$ on flutter speed for CAST 7 by LTRAN2.

different limitations of the two programs, different angles of attack had to be considered: −0.2, 0.0, 0.2, 0.42, 0.6, and 0.8 deg for LTRAN2, and −0.4, 0.0, 0.42, 0.75, 1.0, 1.2, and 1.3 deg for STRANS2/UTRANS2, respectively. Figures 4 and 5 show the steady pressure curves obtained by STRANS2 and LTRAN2, respectively. The obvious discrepancies between the two sets of curves are due to the differences in the two codes which will be discussed in the Concluding Remarks. The corresponding unsteady aerodynamic coefficients obtained by UTRANS2 and LTRAN2 are shown in Tables 1 and 2, respectively.

Based on these coefficients, flutter analysis was conducted and the results are given as plots of flutter speed and corresponding reduced frequency vs angle of attack for various values of the aeroelastic parameters. Detailed results are presented in Ref. 32. Figures 6 and 7 show two typical sets of flutter curves obtained by STRANS2/UTRANS2 and LTRAN2, respectively. Figure 6 shows the effect of angle of attack on flutter speed for three values of airfoil-air mass density ratio (100, 200, and 300). The values for $x_\alpha$, $a_h$, and $\omega_h/\omega_\alpha$ were 0.5, −0.5, and 0.1, respectively. The corresponding results for LTRAN2 are given in Fig. 7. In both figures, the flutter speed increases with the increase in mass ratio. The flutter speed gradually increases with the increase in angle of attack. The increase appears to be more rapid in the neighborhood of $\alpha = 0.8$ deg.

Because of the limitations of both codes, the upper limits of $\alpha$ considered by LTRAN2 and UTRANS2 were 0.8 and 1.3 deg, respectively. In the extra region of higher $\alpha$-values studied by UTRANS2 (see Fig. 6), it appears that the increasing trend of the flutter speed curves becomes more flattened in the neighborhood of the design angle of attack 1.3 deg, indicating that for the values of the parameters chosen, the airfoil is more stable near the original design angle of attack.

### Flutter Analysis of a CAST 7 Supercritical Airfoil

Detailed analysis of a CAST 7 supercritical airfoil (11.9% thickness-to-chord ratio) was conducted by LTRAN2 to study the effects of Mach number on flutter speed for four

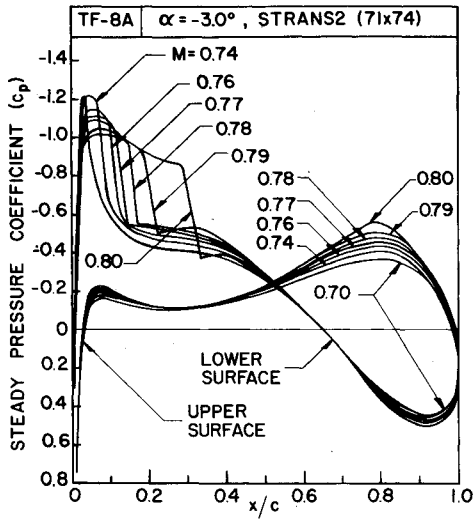


**Fig. 11 Distribution of steady pressure coefficients for TF-8A wing section by STRANS2.**

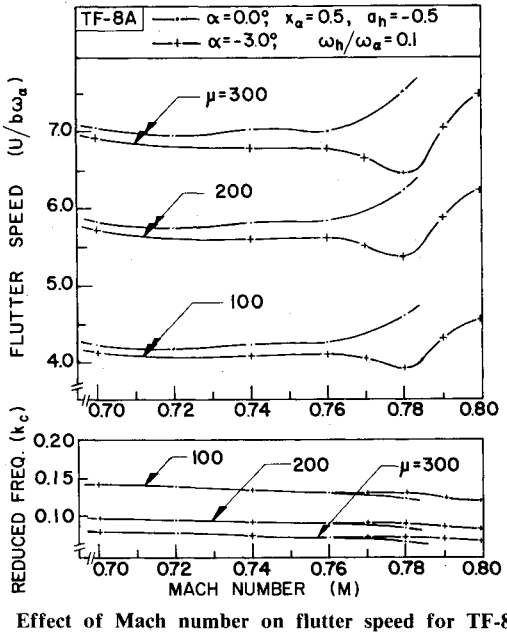


**Fig. 12 Effect of Mach number on flutter speed for TF-8A by STRANS2/UTRANS2.**

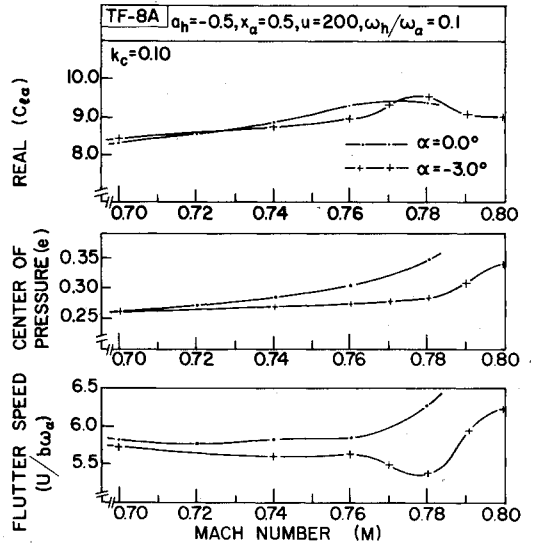


**Fig. 13 Compensation effects of Re ($C_{l\alpha}$) and $e$ on flutter speed for TF-8A by STRANS2/UTRANS2.**

aeroelastic parameters at 0-deg angle of attack. The Mach numbers considered were 0.60, 0.625, 0.65, 0.675, 0.70, 0.71, and 0.72, respectively.

Figure 8 shows the effect of Mach number on the upper and lower surface steady pressure curves obtained by LTRAN2. $M=0.72$ is practically the highest Mach number that can be considered in the present analysis. The corresponding unsteady aerodynamic coefficients are shown in Table 3. Based on these coefficients, the flutter analysis was conducted.

Figure 9 shows the curves of flutter speed and corresponding reduced frequency vs Mach number for three values of airfoil-air mass density ratio (100, 200, and 300). The other aeroelastic parameters $x_\alpha$, $a_\alpha$, and $\omega_h/\omega_\alpha$ were assumed as 0.5, $-0.5$, and 0.1, respectively. In this figure, the flutter speed increases with the increase in airfoil-air mass density ratio. All curves for flutter speed present a dip in the neighborhood of $M=0.71$. The shapes of the dip are more pronounced for higher values of $\mu$. Similar results obtained by varying the other aeroelastic parameters are presented in Ref. 32.

The transonic dip may be explained as the result of the compensating effects of the lift coefficient $C_{l\alpha}$ and the position of center of pressure $e$. Such effects are shown for the CAST 7 airfoil in Fig. 10. In this figure, Re($C_{l\alpha}$) increases with the increase in Mach number and the flutter speed drops at a comparable rate. The $e$ value stays more or less unchanged up to about $M=0.70$. Thereafter, the $e$ value increases noticeably; i.e., the center of pressure moves aft, which increases the flutter speed sharply.

### Flutter Analysis of a TF-8A Wing Section at the 65.3% Semispan Station

The TF-8A supercritical wing was developed by NASA and has been subjected to various aerodynamic and aeroelastic studies.[2,23] In this paper, a flutter analysis of the typical wing section at the 65.3% semispan station (7.9% thickness-to-chord ratio) was undertaken at various Mach numbers by STRANS2/UTRANS2. In a wind-tunnel test,[28] the local angle of attack of this wing section was $-3.0$ deg when corresponding to a zero mean angle of attack of the zero-twist station at the 1-$g$ design condition. Hence, this flutter analysis was performed at $\alpha=-3.0$ deg and also at $\alpha=0.0$ deg for comparison.

Figure 11 shows the upper and lower surface steady pressure curves obtained for the TF-8A wing section for seven Mach numbers (0.70, 0.74, 0.76, 0.77, 0.78, 0.79, and 0.80) at $\alpha=-3.0$ deg by STRANS2. The corresponding unsteady aerodynamic coefficients by UTRANS2 are given in Table 4. Based on these coefficients, flutter analysis was conducted and the effect of Mach number on flutter speed was studied for various values of the aeroelastic parameters.

Figure 12 shows the curves for flutter speed and the corresponding reduced frequency vs Mach number at $\alpha=-3.0$ and 0.0 deg obtained for three airfoil-air mass density ratios (100, 200, and 300). The other aeroelastic parameters $x_\alpha$, $a_h$, and $\omega_h/\omega_\alpha$ were assumed as 0.5, $-0.5$, and 0.1, respectively. In this figure, the flutter speed increases with the increase in mass ratio for both angles of attack. All the three curves for $\alpha=-3.0$ deg present a dip in the neighborhood of $M=0.78$. The dip is more pronounced for higher $\mu$ values. The corresponding curves for $\alpha=0.0$ deg do not show a dip other than having their lowest values between $M=0.72$ and 0.76. Results were obtained by varying the other three aeroelastic parameters and are presented in Ref. 32.

As explained earlier, the transonic dip phenomenon may be explained as a result of the compensating effects of the lift coefficient $C_{l\alpha}$ and the position of center of pressure $e$. Such effects are shown in Fig. 13.

### Time Response Analysis

Aeroelastic time response results for forces and displacements were obtained by simultaneously integrating

the LTRAN2 aerodynamic equations and the structural equations by a direct integration method. One- and two-degree-of-freedom systems were considered for a flat plate and a NACA 64A006 airfoil.

For the flat plate, the time response analysis was performed at $M=0.70$. The results compared well with the corresponding ones obtained by linear aerodynamic theory.

For the NACA 64A006 airfoil pitching about midchord at $M=0.88$, the present time response results compared well with those given in Ref. 17. For the NACA 64A006 airfoil plunging and pitching simultaneously, a neutrally stable response was found when checking a lowest point (at $M=0.85$) on the flutter speed curves obtained previously. The effect of mass ratio on the time response was also studied. Details of this time response analysis are given in Refs. 33 and 34.

## Concluding Remarks

Within the range of aeroelastic parameters considered in this study, the following concluding remarks may be made.

1) The indicial method is computationally more economical than harmonic and time integration methods. The time integration method is from theory more accurate than the indicial and harmonic methods. It can treat shock movement during the unsteady computations.

2) The MBB A-3 airfoil is more stable at design angle of attack than at 0-deg angle of attack. The removal of camber from the MBB A-3 airfoil generally decreases the flutter speed. The aerodynamic and flutter results obtained for the MBB A-3 airfoil without camber and those for the conventional NACA 64A010 airfoil scaled down to 8.9% maximum thickness-to-chord ratio are almost the same.

3) For the case of zero mean angle of attack, all the curves for flutter speed obtained for the MBB A-3 supercritical airfoil showed a dip phenomenon in the neighborhood of the design Mach number $M=0.765$. At $M=0.765$, the flutter speed for the MBB A-3 airfoil increases with the increase in angle of attack. However, this was not the case for the flutter curve given by LTRAN2 for $\omega_h/\omega_\alpha=0.2$. STRANS2/UTRANS2 results indicate that the increasing trend of the flutter speed with the increase in $\alpha$ slows down in the neighborhood of the design angle of attack $\alpha=1.3$ deg.

4) The flutter curves for the CAST 7 supercritical airfoil present a dip around $M=0.71$ and those for the TF 8-A wing section at $\alpha=-3.0$ deg present a dip around $M=0.78$. This seems to indicate that for the supercritical airfoils, the similar but thicker airfoils experience the transonic dip at lower Mach numbers than thinner airfoils. Also, the supercritical airfoils with camber appear to show transonic dips at lower Mach numbers than the symmetric conventional airfoils.

5) Aerodynamic and flutter results obtained by LTRAN2 and STRANS2/UTRANS2 compare well for most of the cases. The comparisons were better for thinner airfoils, lower Mach numbers, and smaller angles of attack. Discrepancies between the results by the two programs may be attributed to the differences in mesh size, the manner in which the shocks are treated in the two respective programs, and the aerodynamic and computational differences between the two programs.

6) In the time response study for the NACA 64A006 airfoil, neutrally stable response was found when checking a lowest point on the flutter speed curve obtained by flutter analysis. The agreement between the two methods, one does not and one does use the principle of linear superposition of airloads, seems to indicate that this principle is valid at least for the values of the parameters assumed in this study.

7) Due to the low frequency approximation used in LTRAN2 and the convergence difficulty encountered in using UTRANS2, the reduced frequencies $k_c$ considered in all cases were limited to be not more than 0.2. The plunge-to-pitch frequency ratio $\omega_h/\omega_\alpha$ had to be held to lower values of 0.1 and 0.2 in most cases. For both programs, convergence and accuracy deteriorated with the increase in Mach number, angle of attack, and thickness of the airfoil.

8) For a more complete understanding of the transonic flutter behavior of conventional and supercritical airfoils, the present limitations on low reduced frequency, small angle of attack, and low Mach number must be relaxed. Viscous effects should be included in the transonic codes. Such developments have been under way.[5-8] More developments in three-dimensional transonic codes and their applications to flutter analysis of full wings are needed. Studies in this direction can be found in Refs. 3, 10, and 24. Experimental flutter trend data are needed to verify the present analytical results.

## Acknowledgments

This three year research was sponsored under Air Force Office of Scientific Research Grant 78-3523. The research was administered by J.J. Olsen and L.J. Huttsell of the Air Force Wright Aeronautical Laboratories. The authors are grateful for many original ideas from J.J. Olsen. They are also grateful for the advice and help from J.J. Olsen, L.J. Huttsell, W.F. Ballhaus, and P.M. Goorjian of NASA Ames Research Center, and S.R. Bland of NASA Langley Research Center.

## References

[1] Ballhaus, W.F. and Bridgeman, J.O., "Numerical Solution Techniques for Unsteady Transonic Problems," AGARD Rept. 679, Paper 16, March 1980.

[2] Ashley, H., "Role of Shocks in the 'Sub-Transonic' Flutter Phenomenon," *Journal of Aircraft,* Vol. 17, March 1980, pp. 187-197.

[3] Traci, R.M., Albano, E.D., and Farr, J.L., "Small Disturbance Transonic Flows About Oscillating Airfoils and Planar Wings," AFFDL-TR-75-100, June 1975.

[4] Ballhaus, W.F. and Goorjian, P.M., "Implicit Finite-Difference Computations of Unsteady Transonic Flows About Airfoils," *AIAA Journal,* Vol. 15, Dec. 1977, pp. 1728-1735.

[5] Houwink, R. and van der Vooren, J., "Results of an Improved Version of LTRAN2 for Computing Unsteady Airloads on Airfoils Oscillating in Transonic Flow," AIAA Paper 79-1553, July 1979.

[6] Rizzetta, D.P. and Yoshihara, H., "Computations of the Pitching Oscillation of a NACA 64A010 Airfoil in the Small Disturbance Limit," AIAA Paper 80-0128, Jan. 1980.

[7] Goorjian, P.M., "Implicit Computations of Unsteady Transonic Flow Governed by the Full Potential Equation in Conservation Form," AIAA Paper 80-0150, Jan. 1980.

[8] Williams, M.H., "Linearization of Unsteady Transonic Flows Containing Shocks," *AIAA Journal,* Vol. 17, April 1979, pp. 394-397.

[9] Yang, T.Y., Striz, A.G., and Guruswamy, P., "Flutter Analysis of Two-Dimensional and Two-Degree-of-Freedom Airfoils in Small-Disturbance Unsteady Transonic Flow," AFFDL-TR-78-202, Dec. 1978.

[10] Borland, C., Rizzetta, D., and Yoshihara, H., "Numerical Solution of Three-Dimensional Unsteady Transonic Flow over Swept Wings," AIAA Paper 80-1369, July 1980.

[11] Experimental Data Base for Computer Program Assessment, Report of the Fluid Dynamics Panel Working Group 04, AGARD-AR-138, May 1979.

[12] Tijdeman, H., "Investigations of the Transonic Flow Around Oscillating Airfoils," National Aerospace Laboratory, The Netherlands, NLR-TR-77090U, Dec. 1977.

[13] Davis, S.S. and Malcolm, G.N., "Experiments in Unsteady Transonic Flow," AIAA Paper 79-0769, April 1979.

[14] Davis, S.S. and Malcolm, G.N., "Unsteady Aerodynamics of Conventional and Supercritical Airfoils," *Proceedings of the AIAA/ASME/ASCE/AHS 21st Structures, Structural Dynamics and Materials Conference,* Seattle, Wash., May 1980, pp. 417-433.

[15] Rizzetta, D.P., *"Transonic Flutter Analysis of a Two-Dimensional Airfoil,"* AFFDL-TM-77-64-FBR, July 1977.

[16] Rizzetta, D.P., *"The Aeroelastic Analysis of a Two-Dimensional Airfoil in Transonic Flow,"* AFFDL-TR-77-126, Dec. 1977; see also, *AIAA Journal,* Vol. 17, Jan. 1979, pp. 26-32.

[17] Ballhaus, W.F. and Goorjian, P.M., "Computation of Unsteady Transonic Flows by the Indicial Method," *AIAA Journal,* Vol. 16, Feb. 1978, pp. 117-124.

[18] McGrew, J.A., Giesing, J.P., Pearson, R.M., Zuruddin, K., Schmidt, M.E., and Kalman, T.P., "Supercritical Wing Flutter," AFFDL-TR-78-37, March 1978.

[19] Mykytow, W.J., "A Brief Overview of Transonic Flutter Problems," *Unsteady Airloads in Separated and Transonic Flow,* AGARD-CP-226, April 1977, pp. 11-1-11-11.

[20] Isogai, K., "On the Transonic-Dip Mechanism of Flutter of a Sweptback Wing," *AIAA Journal,* Vol. 17, July 1979, pp. 793-795.

[21] Isogai, K., "Numerical Study of Transonic Flutter of a Two-Dimensional Airfoil," Technical Report of National Aerospace Laboratory, Chofu, Tokyo, Japan, NAL TR-617T, July 1980.

[22] Hitch, H.P.Y., "Comment on Flutter Analysis of NACA 64A006 Airfoil in Small Disturbance Transonic Flow," see also Yang, T.Y., Guruswamy, P., Striz, A.G., and Olsen, J.J., "Reply by Authors to H.P.Y. Hitch," *Journal of Aircraft,* Vol. 18, Feb. 1981, pp. 158-160.

[23] Farmer, M.G. and Hanson, P.W., "Comparison of Supercritical and Conventional Wing Flutter Characteristics," *Proceedings of the AIAA/ASME/SAE 17th Structures, Structural Dynamics and Materials Conference,* King of Prussia, Pa., April 1976, pp. 608-611; see also, NASA TM X-72837, May 1976.

[24] Eastep, F.E. and Olsen, J.J., "Transonic Flutter Analysis of a Rectangular Wing with Conventional Airfoil Sections," *AIAA Journal,* Vol. 18, Oct. 1980, pp. 1159-1164.

[25] Bisplinghoff, R.L., Ashley, H., and Halfman, R.L., *Aeroelasticity,* Addison-Wesley Publishing Co., Cambridge, Mass., 1955, Sec. 9-2.

[26] Olsen, J.J., Personal Communication.

[27] Olsen, J.J., "AGARD Standard Configurations for Aeroelastic Applications of Transonic Unsteady Aerodynamics, Part III, Candidate Airfoil Data," AFFDL-TM-78-6-FBR, Jan. 1978.

[28] Montoya, L.C. and Banner, R.D., "F-8 Supercritical Wing Flight Pressure, Boundary Layer, and Wake Measurements and Comparisons with Wind Tunnel Data," NASA TM X-3544, June 1977.

[29] Yang, T.Y., Guruswamy, P., Striz, A.G., and Olsen, J.J., "Flutter Analysis of a NACA 64A006 Airfoil in Small Disturbance Transonic Flow," *Journal of Aircraft,* Vol. 17, April 1980, pp. 225-232.

[30] Yang, T.Y., Guruswamy, P., and Striz, A.G., "Flutter Analysis of a Two-Dimensional and Two-Degree-of-Freedom Supercritical Airfoil in Small Disturbance Unsteady Transonic Flow," AFWAL-TR-80-3010, March 1980.

[31] Yang, T.Y., Striz, A.G., and Guruswamy, P., "Flutter Analysis of a Two-Degree-of-Freedom MBB A-3 Supercritical Airfoil in Two-Dimensional Transonic Flow," *Proceedings of the AIAA/ASME/ASCE/AHS 21st Structures, Structural Dynamics and Materials Conference,* Seattle, Wash., May 1980, pp. 434-443; see also, *Journal of Aircraft,* Vol. 18, Oct. 1981, pp. 887-890.

[32] Yang, T.Y., Striz, A.G., and Guruswamy, P., "Flutter Analysis of Two-Dimensional and Two-Degree-of-Freedom MBB A-3, CAST 7, and NASA TF-8A Supercritical Airfoils in Small-Disturbance Unsteady Transonic Flow," AFWAL-TR-81-3004, March 1981.

[33] Yang, T.Y., Guruswamy, P., and Striz, A.G., "Aeroelastic Response Analysis of Two Dimensional Single and Two Degree of Freedom Airfoils in Low-Frequency, Small-Disturbance, Unsteady Transonic Flow," AFFDL-TR-79-3077, June 1979.

[34] Guruswamy, P. and Yang, T.Y., "Aeroelastic Time Response Analysis of Thin Airfoils by Transonic Code LTRAN2," *International Journal of Computers and Fluids,* Vol. 9, Dec. 1981, pp. 409-425.